

Cache-Aided Combination Networks with Interference

Ahmed Roushdy, Abolfazl Seyed Motahari, Mohammed Nafie and
Deniz Gündüz

Abstract

Centralized coded caching and delivery is studied for a radio access combination network (RACN), whereby a set of H edge nodes (ENs), connected to a cloud server via orthogonal fronthaul links with limited capacity, serve a total of K user equipments (UEs) over wireless links. The cloud server is assumed to hold a library of N files, each of size F bits; and each user, equipped with a cache of size $\mu_R NF$ bits, is connected to a distinct set of r ENs each of which equipped with a cache of size $\mu_T NF$ bits, where $\mu_T, \mu_R \in [0, 1]$ are the fractional cache capacities of the UEs and the ENs, respectively. The objective is to minimize the normalized delivery time (NDT), which refers to the worst case delivery latency when each user requests a single distinct file from the library. Three coded caching and transmission schemes are considered, namely the *MDS-IA*, *soft-transfer* and *zero-forcing (ZF)* schemes. MDS-IA utilizes maximum distance separable (MDS) codes in the placement phase and real interference alignment (IA) in the delivery phase. The achievable NDT for this scheme is presented for $r = 2$ and arbitrary fractional cache sizes μ_T and μ_R , and also for arbitrary value of r and fractional cache size μ_T when the cache capacity of the UE is above a certain threshold. The soft-transfer scheme utilizes soft-transfer of coded symbols to ENs that implement ZF over the edge links. The achievable NDT for this scheme is presented for arbitrary r and arbitrary fractional cache sizes μ_T and μ_R . The last scheme utilizes ZF between the ENs and the UEs without the participation of the cloud server in the delivery phase. The achievable NDT for this scheme is presented for an arbitrary value of r when the total cache size at a pair of UE and EN is sufficient to store the whole library, i.e., $\mu_T + \mu_R \geq 1$. The

A. Roushdy is with the Department of Engineering Mathematics and Physics, Faculty of Engineering and the Intelligent Networks Center (WINC), Nile University (email: ahmed.elkordy17@imperial.ac.uk). A. S. Motahari is with the Department of Computer Engineering, Sharif University of Technology (email: motahari@sharif.edu). M. Nafie is with the Electronics and Communications Department, Cairo University (email: mnafie@ieee.org). D. Gündüz is with the Information Processing and Communication Lab, Imperial College London (email: d.gunduz@imperial.ac.uk).

The material in this paper was presented in part at the IEEE Wireless Communications and Networking Conference (WCNC) in Barcelona, Spain, in April 2018.

results indicate that the fronthaul capacity determines which scheme achieves a better performance in terms of the NDT, and the soft-transfer scheme becomes favorable as the fronthaul capacity increases.

Index Terms

Coded caching, interference management, latency, interference alignment, combination networks.

I. INTRODUCTION

Proactively caching is considered a promising solution for the growing network traffic and latency for future communication networks [1]–[5]. A centralized coded proactive caching scheme was introduced in [6], and it is shown to provide significant coding gains with respect to classical uncoded caching. Decentralized coded caching is considered in [7], [8], where each user randomly stores some bits from each file independently of the other users. More recently, coded caching has been extended to wireless radio access networks (RANs), where transmitters and/or receivers are equipped with cache memories. Cache-aided delivery over a noisy broadcast channel is considered in [9] and [10]. Cache-aided delivery from multiple transmitters is considered in [11]–[18]. It is shown in [11] that caches at the transmitters can improve the sum degrees of freedom (DoF) by allowing cooperation among transmitters for interference mitigation. In [12] and [19] this model is extended to an interference network with K_T transmitters and K_R receivers, where both the transmitters and receivers are equipped with cache memories. An achievable scheme exploiting real interference alignment (IA) for the general $K_T \times K_R$ network is proposed in [13], which also considers decentralized caching at the users. An interference network with random topology is considered in [20].

While the above works assume that the transmitter caches are large enough to store all the database, the fog-aided RAN (F-RAN) model [14] allows the delivery of contents from the cloud server to the edge-nodes (ENs) through dedicated fronthaul links. Coded caching for the F-RAN scenario with cache-enabled ENs is studied in [14]. The authors propose a centralized coded caching scheme to minimize the normalized delivery time (NDT), which measures the worst case delivery latency with respect to an interference-free baseline system in the high signal-to-noise ratio (SNR) regime. In [15], the authors consider a wireless fronthaul that enables coded multicasting. In [16], decentralized coded caching is studied for a RAN architecture with two ENs, in which both the ENs and the users have caches. In [17], this model is extended to an arbitrary number of ENs and users. We note that the models in [14]–[17] assume a fully connected

interference network between the ENs and users. A partially connected RAN is studied in [18] from an online caching perspective.

If each EN is connected to a subset of the users through dedicated error free orthogonal links, the corresponding architecture is known as a *combination network*. Coded caching in a combination network is studied in [21]–[23]. In such networks, the server is connected to a set of H relay nodes, which communicate to $K = \binom{H}{r}$ users, such that each user is connected to a distinct set of r relay nodes, where r is referred to as the *receiver connectivity*. The links are assumed to be error- and interference-free. The objective is to determine the minimax link load, defined as the minimum achievable value of the maximum load among all the links (proportional to the download time) and over all possible demand combinations. Note that, although the delivery from the ENs to the users takes place over orthogonal links, that is, there are no multicasting opportunities as in [6], the fact that the messages for multiple users are delivered from the server to each relay through a single link allows coded delivery to offer gains similarly to [6]. The authors of [22] consider a class of combination networks that satisfy the resolvability property, which require H to be divisible by r . A combination network in which both the relays and the users are equipped with caches is presented in [23]. For the case when there are no caches at the relays, the authors are able to achieve the same performance as in [22] without requiring the resolvability property.

In this paper we study the centralized caching problem in a RACN with cache-enabled user equipments (UEs) and ENs, as depicted in Fig. 1. Our work differs from the aforementioned prior works [14]–[17] as we consider a partially connected interference channel from the ENs to the UEs, instead of a fully connected RAN architecture. This may be due to physical constraints that block the signals or the long distance between some of the EN-UE pairs. The network from the server to the UEs, where ENs act as relays for the UEs they serve, is similar to the combination network architecture [21]–[23]; however, we consider interfering wireless links from the ENs to the UEs instead of dedicated links, and study the normalized delivery time in the high SNR regime. The authors in [24] study the NDT for a partially connected $(K + L - 1) \times K$ interference channel with caches at both the transmitters and the receivers, where each receiver is connected to L consecutive transmitters. Our work is different from [24], since we take into consideration the fronthaul links from the server to the ENs, and consider a network topology in which the number of transmitters (ENs in our model) is less than or equal to the number of receivers, which we believe is a more realistic scenario.

We formulate the minimum NDT problem for a given *receiver connectivity* r . Then, we propose three centralized caching and delivery schemes; in particular, the *MDS-IA* scheme that we proposed in our previous work [25], the *soft-transfer* scheme and the *zero-forcing (ZF)* scheme. The MDS-IA scheme exploits real IA to minimize the NDT for receiver connectivity of $r = 2$. We then extend this scheme to an arbitrary receiver connectivity of r assuming a certain cache capacity at the UEs while an arbitrary cache capacity at the ENs. For this scheme, we show that increasing the receiver connectivity for the same number of ENs and UEs will decrease the NDT for the specific cache capacity region studied at the UEs, while the reduction in the NDT depends on the fronthaul capacity. On the other, in the soft-transfer scheme the server delivers quantized channel input symbols to the ENs in order to enable them to implement ZF transmission to the UEs to minimize the NDT for an arbitrary receiver connectivity and cache capacity at both the ENs and the UEs. The ZF scheme is presented when the total cache size at one UE and one EN is sufficient to store the entire library, i.e., $\mu_T + \mu_R \geq 1$, then the cloud server can remain silent during the delivery phase and all users requests can be satisfied by ZF from the ENs to the UEs.

Our results show that the best scheme in terms of the NDT depends on the fronthaul capacity and the cache sizes. For the case when the total cache size of the EN and UE is not sufficient to store the entire library, i.e., $\mu_T + \mu_R < 1$, the MDS-IA scheme achieves a smaller NDT when the fronthaul capacity is relatively limited, while the soft-transfer scheme performs better as the fronthaul capacity increases. On the other hand, when the total cache size of the EN and UE is sufficient to store the entire library, the ZF scheme achieves a smaller NDT than the other proposed schemes when the fronthaul capacity is relatively limited.

The rest of the paper is organized as follows. In Section II, we introduce the system model and the performance measure. In Section III, the main results of the paper are presented. The MDS-IA scheme is presented in Section IV, while the soft-transfer scheme is introduced in Section V. After that, the ZF scheme is presented in Section VI, while the numerical results are presented in section VII. Finally, the paper is concluded in Section VIII.

A. Notation

We denote sets with calligraphic symbols and vectors with bold symbols. The set of integers $\{1, \dots, N\}$ is denoted by $[N]$. The cardinality of set \mathcal{A} is denoted by $|\mathcal{A}|$. We use the function $(x)^+$ to return $\max(x, 0)$.

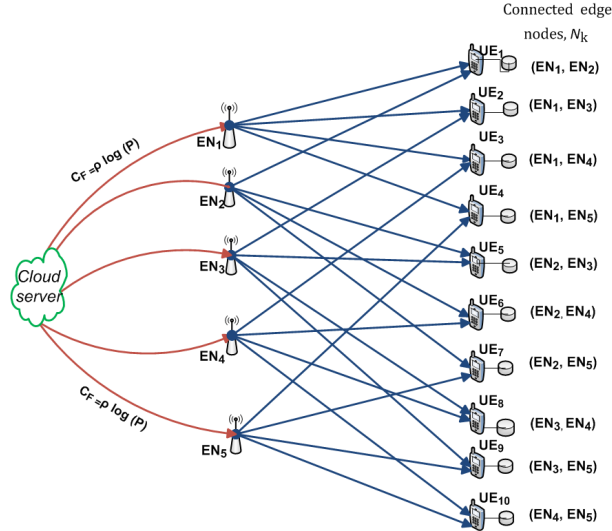


Fig. 1: RACN architecture with receiver connectivity $r = 2$, where $H = 5$ ENs serve $K = 10$ UEs.

II. SYSTEM MODEL AND PERFORMANCE MEASURE

A. System Model

We consider the $H \times K$ RACN architecture as illustrated in Fig. 1, which consists of a cloud server and a set of H ENs, $\mathcal{E} \triangleq \{EN_1, \dots, EN_H\}$, that help the cloud server to serve the requests from a set of K UEs, $\mathcal{U} \triangleq \{UE_1, \dots, UE_K\}$. The cloud is connected to each ENs via orthogonal fronthaul links of capacity C_F bits per symbol, where the symbol refers to a single use of the edge channel from the ENs to the UEs. The edge network from the ENs to the users is a partially connected interference channel, where $UE_k \in \mathcal{U}$ is connected to a distinct set of r ENs, where $r < H$ is referred to as the *receiver connectivity*. The number of UEs is $K = \binom{H}{r}$, which means that $H \leq K$. In this architecture, $EN_i, i \in [H]$, is connected to $L = \binom{H-1}{r-1} = \frac{rK}{H}$ UEs.

The cloud server holds a library of N files, $\mathcal{W} \triangleq \{W_1, \dots, W_N\}$, each of size F bits. We assume that the UEs request files from this library only. Each UE is equipped with a cache memory of size $\mu_R NF$ bits, while each EN is equipped with a cache memory of size $\mu_T NF$, where $\mu_T, \mu_R \in [0, 1]$, are the fractional cache capacities of the UEs and the ENs, respectively. We define two parameters, $t_U = \mu_R K$ and $t_E = \mu_T L$, where the former is the normalized cache capacity (per file) available across all the UEs, while the latter is the normalized cache capacity of the UEs connected to a particular edge node. We denote the set of UEs connected to EN_i by \mathcal{K}_i , where $|\mathcal{K}_i| = L$, and the set of ENs connected to UE_k by \mathcal{N}_k , where $|\mathcal{N}_k| = r$. We will

use the function $\text{Index}(i, k) : [H] \times [K] \rightarrow [L] \cup \epsilon$, which returns ϵ if UE_k is not served by EN_i , and otherwise returns the relative order of UE_k among the L UEs served by EN_i with the assumption that the L UEs in \mathcal{K}_i are sorted in ascending order. For example, in Fig. 1, we have $\mathcal{K}_1 = \{1, 2, 3, 4\}$, $\mathcal{K}_3 = \{2, 5, 8, 9\}$ and

$$\begin{aligned} \text{Index}(1, 2) &= 2, & \text{Index}(1, 3) &= 3, & \text{Index}(1, 5) &= \epsilon, \\ \text{Index}(3, 2) &= 1, & \text{Index}(3, 5) &= 2, & \text{Index}(3, 1) &= \epsilon. \end{aligned}$$

The system operates in two phases: a *placement phase* and a *delivery phase*. The placement phase takes place when the traffic load is low, and the network nodes are given access to the entire library \mathcal{W} . UE_k , $k \in [K]$, and EN_i , $i \in [H]$, are then able to fill their caches using the library without any prior knowledge of the future demands or the channel coefficients. Let Z_k and U_i , $k \in [K]$, $i \in [H]$, denote the cache contents of UE_k and EN_i at the end of the placement phase, respectively. We consider centralized placement; that is, the cache contents of UEs and the ENs, denoted by Z_1, \dots, Z_K , are coordinated jointly.

In the delivery phase, UE_k , $k \in [K]$, requests file W_{d_k} from the library, $d_k \in [N]$. We define $\mathbf{d} = [d_1, \dots, d_K] \in [N]^K$ as the demand vector. Once the demands are received, the cloud server sends message $\mathbf{G}_i = (G_i(t))_{t=1}^{T_F}$ of blocklength T_F to EN_i , $i \in [H]$, via the fronthaul link. This message is limited to $T_F C_F$ bits to guarantee correct decoding at EN_i with high probability. In this paper, we consider half-duplex ENs; that is, ENs start transmitting only after receiving their messages from the cloud server. This is called *serial transmission* in [14], and the overall latency is the sum of the latencies in the fronthaul and the edge connections. EN_i has an encoding function that maps the cache contents U_i , fronthaul message \mathbf{G}_i , the demand vector \mathbf{d} , and the channel coefficients $\mathbf{H} \triangleq \{h_{k,i}\}_{k \in [K], i \in [H]}$, where $h_{k,i}$ denotes the complex channel gain from EN_i to UE_k , to a channel input vector $\mathbf{V}_i = (V_i(t))_{t=1}^{T_E}$ of blocklength T_E , which must satisfy an average power constraint of \mathbf{P} , i.e., $E[\frac{1}{T_E} \mathbf{V}_i \mathbf{V}_i^T] \leq \mathbf{P}$. UE_k decodes its requested file as \hat{W}_{d_k} by using its cache contents Z_k , the received signal $\mathbf{Y}_k = (Y_k(t))_{t=1}^{T_E}$, as well as its knowledge of the channel gain matrix \mathbf{H} and the demand vector \mathbf{d} . We have

$$Y_k(t) = \sum_{i \in \mathcal{N}_k} h_{k,i} V_i(t) + n_k(t), \quad (1)$$

where $n_k(t) \sim \mathcal{CN}(0, 1)$ denotes the independent additive complex Gaussian noise at the k th user. The channel gains are independent and identically distributed (i.i.d.) according to a continuous distribution, and remain constant within each transmission interval. Similarly to [11]–[15], we

assume that perfect channel state information is available at all the terminals of network. The probability of error for a coding scheme, consisting of the cache placement, cloud encoding, EN encoding, and user decoding functions, is defined as

$$P_e = \max_{\mathbf{d} \in [N]^K} \max_{k \in [K]} P_e(\hat{W}_{d_k} \neq W_{d_k}), \quad (2)$$

which is the worst-case probability of error over all possible demand vectors and all the users. We say that a coding scheme is *feasible*, if we have $P_e \rightarrow 0$ when $F \rightarrow \infty$, for almost all realizations of the channel matrix \mathbf{H} .

B. Performance Measure

We will consider *the normalized delivery time (NDT)* in the high SNR regime [26] as the performance measure. Note that the capacity of the edge network scales with the SNR. Hence, to make sure that the fronthaul links do not constitute a bottleneck, we let $C_F = \rho \log P$, where ρ is called the *fronthaul multiplexing gain*. The multiplexing gain is the pre-log term in the capacity expression [27], [28], and an important indicator of the capacity behaviour in the high SNR regime. For given μ_T , μ_R and fronthaul multiplexing gain ρ , we say that $\delta(\mu_R, \mu_T, \rho)$ is an *achievable* NDT if there exists a sequence of feasible codes that satisfy

$$\delta(\mu_R, \mu_T, \rho) = \lim_{P, F \rightarrow \infty} \sup \frac{(T_F + T_E) \log P}{F}. \quad (3)$$

We additionally define the fronthaul NDT as

$$\delta_F(\mu_R, \mu_T, \rho) = \lim_{P, F \rightarrow \infty} \sup \frac{T_F \log P}{F}, \quad (4)$$

and the edge NDT as

$$\delta_E(\mu_R, \mu_T, \rho) = \lim_{P, F \rightarrow \infty} \sup \frac{T_E \log P}{F}, \quad (5)$$

such that the end-to-end NDT is the sum of the fronthaul and edge NDTs. We define the minimum NDT for a given (μ_R, μ_T, ρ) tuple as

$$\delta^*(\mu_R, \mu_T, \rho) = \inf \{ \delta(\mu_R, \mu_T, \rho) : \delta(\mu_R, \mu_T, \rho) \text{ is achievable} \}.$$

III. MAIN RESULT

The main results of the paper are stated in the following theorems.

Theorem 1. *For an $H \times K$ RACN architecture, with fractional cache capacities of μ_R and μ_T , fronthaul multiplexing gain $\rho \geq 0$, number of files $N \geq K$, and considering centralized cache placement, the following NDT is achievable by the MDS-IA scheme for integer values of t_E :*

$$\delta_{\text{MDS-IA}}(\mu_R, \mu_T, \rho) = \frac{L - t_E}{r} \left[\frac{r-1}{L} + \frac{1}{t_E+1} \left(1 + \frac{(1 - \mu_T r)^+}{\rho} \right) \right] \quad (6)$$

for a receiver connectivity of $r = 2$, or for arbitrary receiver connectivity when $t_E \geq L - 2$.

Theorem 2. *For the same RACN architecture, the following NDT is achievable by the soft-transfer scheme for integer values of t_U*

$$\delta_{\text{soft}}(\mu_R, \mu_T, \rho) = (K - t_U) \left[\frac{1}{\min\{H + t_U, K\}} + \frac{(1 - \mu_T)}{H\rho} \right]. \quad (7)$$

Theorem 3. *For the same RACN architecture with $\mu_R + \mu_T \geq 1$ the following NDT is achievable by the ZF scheme for integer values of t_R where $t_R = \frac{(\mu_R + \mu_T - 1)K}{\mu_T}$:*

$$\delta_{\text{ZF}}(\mu_R, \mu_T, \rho) = \left(\frac{K - t_R}{\min\{H + t_R, K\}} \right) \mu_T. \quad (8)$$

Remark 1. *The achievable NDT $\delta(\mu_T, \mu_R, \rho)$ is a convex function of μ_T and μ_R for every value of $\rho \geq 0$ [14]. For any two (μ_T^1, μ_R^1) and (μ_T^2, μ_R^2) pairs, convex combination of the corresponding achievable NDT values can be achieved through memory and time sharing. This would require dividing each of the files in the library into two parts, which have the normalized cache capacities as specified in these pairs. Then the delivery schemes specified for these two achievable points are used sequentially in a time-division manner. Hence, for a given μ_T , when t_E is not an integer for the MDS-IA scheme, or t_U is not integer for the soft-transfer scheme, or t_R is not integer for the ZF scheme, we can write $\mu_R = \alpha\mu_R^1 + (1 - \alpha)\mu_R^2$ for some $\alpha \in [0, 1]$, where μ_R^1 and μ_R^2 are two values that lead to integer normalized cache capacities t_E , t_U , or t_R , with $\mu_R^1 > \mu_R^2$. By applying memory time-sharing as in [14], the following NDT is achievable*

$$\delta(\mu_R, \mu_T, \rho)|_{\text{M-sharing}} = \alpha\delta(\mu_R^1, \mu_T, \rho) + (1 - \alpha)\delta(\mu_R^2, \mu_T, \rho). \quad (9)$$

Remark 2. *For the same RACN architecture with $\mu_R + \mu_T \geq 1$ and $\rho \leq \rho_{\text{th}}$, where*

$$\rho_{\text{th}} \triangleq \frac{(1 - \mu_T r)^+ \left(\delta_2 + \frac{(1-\alpha)}{\alpha} \delta_1 \right)}{\left(\frac{K}{\min\{H, K\}} \right) \frac{\mu_T r}{\alpha} - \delta_2 \left((r-1)(\mu_R^2 + \frac{1}{L}) + 1 \right) - \delta_1 \left(\frac{1}{\alpha} - 1 \right) \left((r-1)(\mu_R^1 + \frac{1}{L}) + 1 \right)}, \quad (10)$$

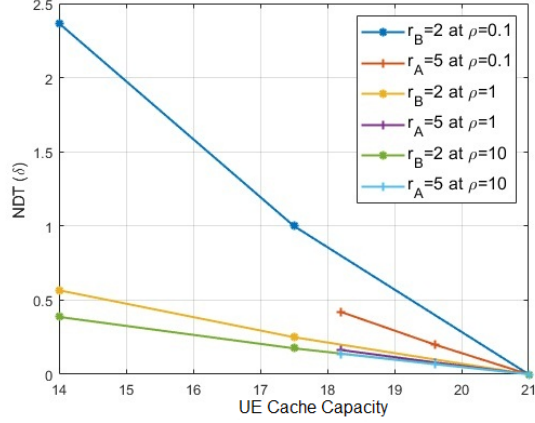


Fig. 2: Comparison of the achievable NDT for a 7×21 RACN architecture with library $N = 21$ files for different receiver connectivity and fronthaul multiplexing gains when there is no cache memory at the ENs.

with $\delta_i = \frac{1-\mu_R^i}{\mu_R^i + \frac{1}{L}}$, for $i = 1, 2$, while μ_R^1 , μ_R^2 and α can be calculated using memory sharing, the ZF scheme achieves a smaller NDT than the other schemes. This is due to the fact that when the fronthaul multiplexing gain is small, it is better to avoid using the fronthaul links.

Remark 3. From Theorem 1 Eqn. (6), when $r \geq 2$, the NDT achieved by the MDS-IA scheme is given by

$$\delta_{\text{MDS-IA}}(\mu_R, \mu_T, \rho) = \begin{cases} \frac{2}{r} \left(\frac{r-1}{L} + \frac{1}{L-1} \left(1 + \frac{(1-\mu_T r)^+}{\rho} \right) \right), & t_E = L - 2 \\ \frac{1}{L} \left(1 + \frac{(1-\mu_T r)^+}{\rho r} \right), & t_E = L - 1 \end{cases}$$

Consider two different RACN architectures with H ENs, denoted by RACN-A and RACN-B, with receiver connectivities r_A and r_B , respectively, where $r_A + r_B = H$ and $r_A \geq r_B$. The two networks have the same number of UEs $K = \binom{r_A+r_B}{r_A} = \binom{r_A+r_B}{r_B}$, but the number of UEs each EN connects to is different, and is given by $L_x = \frac{K}{H} r_x$, $x \in \{A, B\}$. We illustrate the achievable NDT performance of the MDS-IA scheme in a 7×21 RACN in Fig. 2 setting $r_A = 5$ and $r_B = 2$ with no cache memory at the ENs for different fronthaul multiplexing gains. We observe from the figure that, with the same UE cache capacity the achievable NDT of network RACN-A is less than or equal to that of network RACN-B, and the gap between the two increases as the fronthaul multiplexing gain decreases. This suggests that the increased connectivity helps in reducing the NDT despite potentially increasing the interference as well, and the gap between the

two achievable NDTs for RACN-A and RAN-B becomes negligible as the fronthaul multiplexing gain increases, i.e., $\rho \rightarrow \infty$.

IV. MDS-IA SCHEME

We first present the MDS-IA scheme without cache memories at the ENs. Afterwards, we will extend the results to the case with cache memories at the ENs.

A. MDS-IA Scheme without Cache Memories at the ENs

1) **Cache Placement Phase:** We use the placement scheme proposed in [23], where the cloud server divides each file into r equal-size non-overlapping subfiles. Then, it encodes the subfiles using an (H, r) maximum distance separable (MDS) code [29]. The resulting coded chunks, each of size F/r bits, are denoted by f_n^i , where n is the file index and $i \in [H]$ is the index of the coded chunk. EN_i will act as an edge server for the encoded chunk f_n^i , $i \in [H]$. Note that, thanks to the MDS code, any r encoded chunks are sufficient to reconstruct a file.

Each encoded chunk f_n^i is further divided into $\binom{L}{t_E}$ equal-size non-overlapping pieces, each of which is denoted by $f_{n,\mathcal{T}}^i$, where $\mathcal{T} \subseteq [L]$, $|\mathcal{T}| = t_E$. The pieces $f_{n,\mathcal{T}}^i$, $\forall n$, are stored in the cache memory of UE_k if $k \in \mathcal{K}_i$ and $\text{Index}(i, k) \in \mathcal{T}$; that is, the pieces of chunk i , $i \in [H]$, are stored by the L UEs connected to EN_i . At the end of the placement phase, each user stores $Nr \binom{L-1}{t_E-1}$ pieces, each of size $\frac{F}{r \binom{L}{t_E}}$ bits, which sum up to $\mu_R N F$ bits, satisfying the memory constraint with equality. We will next illustrate the placement phase through an example.

Example 1. Consider the RACN depicted in Fig. 1, where $H = 5$, $K = N = 10$, $r = 2$ and $L = 4$. The cloud server divides each file into $r = 2$ subfiles. These subfiles are then encoded using a $(5, 2)$ MDS code. As a result, there are 5 coded chunks, denoted by f_n^i , $n \in [10]$, $i \in [5]$, each of size $F/2$ bits. For $t_E = 1$, i.e., $\mu_R = 1/L$, each encoded chunk f_n^i is further divided into $\binom{L}{t_E} = 4$ pieces $f_{n,\mathcal{T}}^i$, where $\mathcal{T} \subseteq [4]$ and $|\mathcal{T}| = t_E = 1$. Cache contents of each user are listed in TABLE I. Observe that each user stores two pieces of the encoded chunks of each file for a total of 10 files, i.e., $\frac{5}{2}F$ bits, which satisfies the memory constraint.

2) **Delivery Phase:** The delivery phase is carried out in two steps. The first step is the delivery from the cloud server to the ENs, and the second step is the delivery from the ENs to the UEs.

User	UE ₁	UE ₂	UE ₃	UE ₄	UE ₅	UE ₆	UE ₇	UE ₈	UE ₉	UE ₁₀
Cache Contents	$f_{n,1}^1, f_{n,1}^2$	$f_{n,2}^1, f_{n,1}^3$	$f_{n,3}^1, f_{n,1}^4$	$f_{n,4}^1, f_{n,1}^5$	$f_{n,2}^2, f_{n,2}^3$	$f_{n,3}^2, f_{n,2}^4$	$f_{n,4}^2, f_{n,2}^5$	$f_{n,3}^3, f_{n,3}^4$	$f_{n,4}^3, f_{n,3}^5$	$f_{n,4}^4, f_{n,4}^5$

TABLE I: Cache contents after the placement phase for the RACN scenario considered in Example 1, where $K = N = 10$, $r = 2$, $L = 4$, $t_E = 1$ and $\mu_R = \frac{1}{4}$.

EN ₁	EN ₂	EN ₃	EN ₄	EN ₅
$\mathbf{X}_1^{1,2} = f_{1,2}^1 + f_{2,1}^1$	$\mathbf{X}_2^{1,2} = f_{1,2}^2 + f_{5,1}^2$	$\mathbf{X}_3^{1,2} = f_{2,2}^3 + f_{5,1}^3$	$\mathbf{X}_4^{1,2} = f_{3,2}^4 + f_{6,1}^4$	$\mathbf{X}_5^{1,2} = f_{4,2}^5 + f_{7,1}^5$
$\mathbf{X}_1^{1,3} = f_{1,3}^1 + f_{3,1}^1$	$\mathbf{X}_2^{1,3} = f_{1,3}^2 + f_{6,1}^2$	$\mathbf{X}_3^{1,3} = f_{2,3}^3 + f_{8,1}^3$	$\mathbf{X}_4^{1,3} = f_{3,3}^4 + f_{8,1}^4$	$\mathbf{X}_5^{1,3} = f_{4,3}^5 + f_{9,1}^5$
$\mathbf{X}_1^{1,4} = f_{1,4}^1 + f_{4,1}^1$	$\mathbf{X}_2^{1,4} = f_{1,4}^2 + f_{7,1}^2$	$\mathbf{X}_3^{1,4} = f_{2,4}^3 + f_{9,1}^3$	$\mathbf{X}_4^{1,4} = f_{3,4}^4 + f_{10,1}^4$	$\mathbf{X}_5^{1,4} = f_{4,4}^5 + f_{10,1}^5$
$\mathbf{X}_1^{2,3} = f_{2,3}^1 + f_{3,2}^1$	$\mathbf{X}_2^{2,3} = f_{5,3}^2 + f_{6,2}^2$	$\mathbf{X}_3^{2,3} = f_{5,3}^3 + f_{8,2}^3$	$\mathbf{X}_4^{2,3} = f_{6,3}^4 + f_{8,2}^4$	$\mathbf{X}_5^{2,3} = f_{7,3}^5 + f_{9,2}^5$
$\mathbf{X}_1^{2,4} = f_{2,4}^1 + f_{4,2}^1$	$\mathbf{X}_2^{2,4} = f_{5,4}^2 + f_{7,2}^2$	$\mathbf{X}_3^{2,4} = f_{5,4}^3 + f_{9,2}^3$	$\mathbf{X}_4^{2,4} = f_{6,4}^4 + f_{10,2}^4$	$\mathbf{X}_5^{2,4} = f_{7,4}^5 + f_{10,2}^5$
$\mathbf{X}_1^{3,4} = f_{3,4}^1 + f_{4,3}^1$	$\mathbf{X}_2^{3,4} = f_{6,4}^2 + f_{7,3}^2$	$\mathbf{X}_3^{3,4} = f_{8,4}^3 + f_{9,3}^3$	$\mathbf{X}_4^{3,4} = f_{8,4}^4 + f_{10,3}^4$	$\mathbf{X}_5^{3,4} = f_{9,4}^5 + f_{10,3}^5$

TABLE II: The data delivered from the cloud server to each EN for Example 1.

Step 1: Delivery from the cloud server to the ENs For each $(t_E + 1)$ -element subset \mathcal{S} of $[L]$, i.e., $\mathcal{S} \subseteq [L]$ and $|\mathcal{S}| = t_E + 1$, the cloud server will deliver the following message to EN_{*i*}:

$$\mathbf{X}_i^{\mathcal{S}} \triangleq \bigoplus_{k:k \in \mathcal{K}_i, \text{Index}(i,k) \in \mathcal{S}} f_{d_k, \mathcal{S} \setminus \text{Index}(i,k)}^i \quad (11)$$

Overall, for given \mathbf{d} , the following set of messages will be delivered to EN_{*i*}

$$\{\mathbf{X}_i^{\mathcal{S}} : \mathcal{S} \subseteq [L], |\mathcal{S}| = t_E + 1\}, \quad (12)$$

which makes a total of $\binom{L}{t_E+1} \frac{F}{r \binom{L}{t_E}}$ bits. The fronthaul NDT from the cloud server to the ENs is then given by

$$\delta_F(\mu_R, \mu_T, \rho) = \frac{\binom{L}{t_E+1}}{r \binom{L}{t_E}} \rho = \frac{L - t_E}{(t_E + 1)r\rho}. \quad (13)$$

The message to be delivered to each EN in Example 1 is given in TABLE II, and we have $\delta_F(\frac{1}{4}, 0, \rho) = \frac{3}{4\rho}$.

The next step deals with the delivery from the ENs to the UEs over the partially connected interference channel. This is the main distinction of our work from [23], where the authors assume orthogonal links from the relay nodes (ENs in our model) to UEs. Hence, the relay nodes simply transmit coded multicast messages $\mathbf{X}_i^{\mathcal{S}}$ over orthogonal links to their intended receivers. In our scheme, in order to manage the interference between the transmitters. We use real interference alignment as explained in the sequel.

Algorithm 1: Generator for \mathbf{A} , \mathbf{B} and \mathbf{C} Matrices

```

1:  $\mathbf{A} = [], \mathbf{B} = [], \mathbf{C} = [], g = 0$ 
2: FOR  $k = 1, \dots, K$ 
3:   FOR  $j = 1, \dots, I$ 
4:      $g = g + 1$ 
5:     FOR  $i = 1, \dots, r$ 
6:        $\mathbf{B}_g \leftarrow [\mathbf{B}_g \ \mathbf{X}_k(j, i)]$ 
7:       Find  $\mathcal{J}_i$ : set of other UEs receiving the same
8:       interference signal  $\mathbf{X}_k(j, i)$ ,  $|\mathcal{J}_i| = (L - |S| - 1)$ .      Sort UEs in  $\mathcal{J}_i$  in ascending order.
9:       For each user in  $\mathcal{J}_i$ , find interference vector  $\mathbf{x}_k^q$ ,      s.t.  $\text{UE}_k \in \mathcal{J}_i$  and  $\mathbf{X}_k(j, i) \notin \mathbf{x}_k^q$ .
10:       $\mathbf{Q}_i \leftarrow$  set of vectors  $\mathbf{x}_k^q$ 
11:    END FOR
12:    If  $|\mathcal{J}_i| \geq 1$ 
13:      FOR  $R = 1, \dots, |\mathcal{J}_i|$ 
14:        FOR  $e = 1, \dots, |\mathbf{Q}_1(:, R)|$ 
15:          FOR  $c = 1, \dots, |\mathbf{Q}_2(:, R)|$ 
16:            IF  $\mathbf{Q}_1(e, R) = \mathbf{Q}_2(c, R)$ 
17:               $\mathbf{B}_g = [\mathbf{B}_g \ \mathbf{Q}_1(e, R)]$ 
18:              Go to 21, i.e., next iteration of  $R$ .
19:            END IF
20:          END FOR
21:        END FOR
22:      END FOR
23:    END IF     $\mathbf{C}_g \leftarrow \bigcup_{k: \hat{S} \in \mathbf{X}_k} \mathbf{u}_k$ , for  $\hat{S} \subseteq \mathbf{B}_g$ , where  $|\hat{S}| = r$ 
24:    FOR  $e = 1, \dots, |\mathbf{C}_g|$ 
25:      FOR  $i = 1, \dots, r$ 
26:         $\mathbf{A}_g = [\mathbf{A}_g \ h_{\mathbf{C}_g(e), \mathcal{N}_{\mathbf{C}_g(e)}(i)}]$ 
27:      END FOR
28:    END FOR
29:    Remove interference signals in  $\mathbf{B}_g$  from  $(\mathbf{X}_k)_{k=1}^K$ 
30:     $\mathcal{J}_i = [] \ \mathbf{Q}_i = []$  for  $i = 1, \dots, r$ 
31:
32:  END FOR
33: END FOR

```

Step 2 : Delivery from the ENs to UE_k , $k \in [K]$, aims at delivering the following set of

\mathbb{X}_1	\mathbb{X}_2	\mathbb{X}_3	\mathbb{X}_4	\mathbb{X}_5	\mathbb{X}_6	\mathbb{X}_7	\mathbb{X}_8	\mathbb{X}_9	\mathbb{X}_{10}
$\mathbf{X}_1^{2,3} \mathbf{X}_2^{2,3}$	$\mathbf{X}_1^{1,3} \mathbf{X}_3^{2,3}$	$\mathbf{X}_1^{1,2} \mathbf{X}_4^{2,3}$	$\mathbf{X}_1^{1,2} \mathbf{X}_5^{2,3}$	$\mathbf{X}_2^{1,3} \mathbf{X}_3^{1,3}$	$\mathbf{X}_2^{1,2} \mathbf{X}_4^{1,3}$	$\mathbf{X}_2^{1,2} \mathbf{X}_5^{1,3}$	$\mathbf{X}_3^{1,2} \mathbf{X}_4^{1,2}$	$\mathbf{X}_3^{1,2} \mathbf{X}_5^{1,4}$	$\mathbf{X}_4^{1,2} \mathbf{X}_5^{1,2}$
$\mathbf{X}_1^{2,4} \mathbf{X}_2^{2,4}$	$\mathbf{X}_1^{1,4} \mathbf{X}_3^{2,4}$	$\mathbf{X}_1^{1,4} \mathbf{X}_4^{2,4}$	$\mathbf{X}_1^{1,3} \mathbf{X}_5^{2,4}$	$\mathbf{X}_2^{1,4} \mathbf{X}_3^{1,4}$	$\mathbf{X}_2^{1,4} \mathbf{X}_4^{1,4}$	$\mathbf{X}_2^{1,3} \mathbf{X}_5^{1,4}$	$\mathbf{X}_3^{1,4} \mathbf{X}_4^{1,4}$	$\mathbf{X}_3^{1,3} \mathbf{X}_5^{1,4}$	$\mathbf{X}_4^{1,3} \mathbf{X}_5^{1,3}$
$\mathbf{X}_1^{3,4} \mathbf{X}_2^{3,4}$	$\mathbf{X}_1^{2,4} \mathbf{X}_3^{3,4}$	$\mathbf{X}_1^{3,4} \mathbf{X}_4^{3,4}$	$\mathbf{X}_1^{2,3} \mathbf{X}_5^{3,4}$	$\mathbf{X}_2^{3,4} \mathbf{X}_3^{3,4}$	$\mathbf{X}_2^{2,4} \mathbf{X}_4^{3,4}$	$\mathbf{X}_2^{2,3} \mathbf{X}_5^{3,4}$	$\mathbf{X}_3^{2,4} \mathbf{X}_4^{2,4}$	$\mathbf{X}_3^{2,3} \mathbf{X}_5^{2,4}$	$\mathbf{X}_4^{2,3} \mathbf{X}_5^{2,3}$

TABLE III: The interference matrices at the UEs of Example 1.

messages:

$$\mathcal{M}_k = \bigcup_{\substack{i, \mathcal{S}: i \in \mathcal{N}_k, \mathcal{S} \subseteq [L], \\ |\mathcal{S}| = t_E + 1, \text{Index}(i, k) \in \mathcal{S}}} X_i^{\mathcal{S}}, \quad (14)$$

where $|\mathcal{M}_k| = r \binom{L-1}{t_E}$. On the other hand, the transmission of the following messages interfere with the delivery of the messages in \mathcal{M}_k :

$$\mathcal{I}_k = \bigcup_{\substack{i, \mathcal{S}: i \in \mathcal{N}_k, \mathcal{S} \subseteq [L], \\ |\mathcal{S}| = t_E + 1, \text{Index}(i, k) \notin \mathcal{S}}} X_i^{\mathcal{S}}. \quad (15)$$

Each $X_i^{\mathcal{S}} \in \mathcal{I}_k$ causes interference at $L - |\mathcal{S}|$ UEs, including UE $_k$. Hence, the total number of interfering signals at UE $_k$ from the ENs in \mathcal{N}_k is rI , where $I \triangleq \binom{L}{t_E + 1} - \binom{L-1}{t_E}$ is the number of interfering signals from each EN connected to UE $_k$.

We enumerate the ENs in \mathcal{N}_k , $k \in [K]$, such that $\mathcal{N}_k(q)$ is the q -th element in \mathcal{N}_k in ascending order. At UE $_k$, $k \in [K]$, we define the *interference matrix* \mathbb{X}_k to be an $I \times r$ matrix whose columns are denoted by $\{\mathbf{x}_k^q\}_{q=1}^r$, where the q -th column \mathbf{x}_k^q represents the interference caused by a different EN in $\mathcal{N}_k(q)$. For each column vector \mathbf{x}_k^q , we sort the set of interfering signals \mathcal{I}_k for $i = \mathcal{N}_k(q)$ in ascending order. In Example 1, we have $\mathcal{N}_1(1) = \text{EN}_1$, $\mathcal{N}_1(2) = \text{EN}_2$, etc., and the interference matrices are shown in TABLE III. We will use real IA, presented in [30] and extended to complex channels in [31], for the delivery from the ENs to the UEs to align each of the r interfering signals in \mathcal{I}_k , one from each EN, in the same subspace. We define \mathbb{A} , \mathbb{B} and \mathbb{C} to be the basis matrix, i.e., function of the channel coefficients, the data matrix and user matrix, respectively, where the dimensions of these matrices are $G \times r \binom{r+L-|S|-1}{r}$, $G \times (r+L-|S|-1)$ and $G \times \binom{r+L-|S|-1}{r}$, respectively, where $G = \binom{H}{t_E + 1}$. We denote the rows of these matrices by \mathbb{A}_g , \mathbb{B}_g and \mathbb{C}_g , respectively, where $g \in [G]$. The row vectors $\{\mathbb{A}_g\}_{g=1}^G$ are used to generate the set of monomials $\mathcal{G}(\mathbb{A}_g)_{g=1}^G$. Note that, the function $\mathcal{T}(u)$ defined in [11] corresponds to $\mathcal{G}(\mathbb{A}_g)$ in our notation. The set $\mathcal{G}(\mathbb{A}_g)_{g=1}^G$ is used as the transmission directions for the modulation constellation \mathbb{Z}_Q [11] for the whole network. In other words, each row data vector \mathbb{B}_g will use

the set $\mathcal{G}(\mathbb{A}_g)$ as the transmission directions of all its data to align all the r interfering signals from \mathbb{B}_g in the same subspace at $\text{UE}_k \in \mathbb{C}_g$, if these r signals belong to \mathbb{X}_k .

We next explain matrix \mathbb{C} more clearly. For each $\hat{S} \subseteq \mathbb{B}_g$ with $|\hat{S}| = r$, there will be a user at which these data will be aligned in the same subspace, i.e., $|\mathbb{C}_g| = \binom{r+L-|\hat{S}|-1}{r}$. The row \mathbb{C}_g consists of UE_k , where $\hat{S} \in \mathbb{X}_k$.

We employ Algorithm 1 to obtain matrices \mathbb{A} , \mathbb{B} and \mathbb{C} for a receiver connectivity of $r = 2$, and for arbitrary receiver connectivity when $t_E = L - 2$. In Example 1, the three matrices are given as follows:

Generating the first rows for \mathbb{A} , \mathbb{B} and \mathbb{C} Matrices in Example 1

```

1: FOR  $k = 1$  and  $j = 1$ 
2:   FOR  $i = 1$ 
3:      $\mathbb{B}_1 = [\mathbf{X}_1^{2,3}]$ 
4:      $\mathcal{J}_1 = [\text{UE}_4]$  and  $\mathbb{Q}_1 = \begin{pmatrix} \mathbf{X}_5^{2,3} \\ \mathbf{X}_5^{2,4} \\ \mathbf{X}_5^{3,4} \end{pmatrix}$ ,
5:   FOR  $i = 2$ 
6:      $\mathbb{B}_1 = [\mathbf{X}_1^{2,3} \mathbf{X}_2^{2,3}]$ 
7:      $\mathcal{J}_2 = [\text{UE}_7]$  and  $\mathbb{Q}_2 = \begin{pmatrix} \mathbf{X}_5^{1,3} \\ \mathbf{X}_5^{1,4} \\ \mathbf{X}_5^{3,4} \end{pmatrix}$ ,
8:   FOR  $R = 1$ 
9:     The two loops in line 14 and 15 in Algorithm 1 are used to find the common message in the 2 sets  $\mathbb{Q}_1$  and  $\mathbb{Q}_2$ 
10:     $\mathbb{Q}_1(1, 3) = \mathbb{Q}_2(1, 3)$ 
11:     $\mathbb{B}_1 = [\mathbf{X}_1^{2,3} \ \mathbf{X}_2^{2,3} \ \mathbf{X}_5^{3,4}]$ 
12:     $\mathbb{C}_1 = [\text{UE}_1 \ \text{UE}_4 \ \text{UE}_5]$ 
13:    FOR  $e = 1, \dots, 3$ 
14:      FOR  $i = 1, \dots, 2$ 
15:         $\mathbb{A}_1 = [\mathbb{A}_1 \ h_{\mathbb{C}_1(e), \mathcal{N}_{\mathbb{C}_1(e)}(i)}]$ 
16:      END FOR
17:    END FOR
18:     $\mathbb{A}_1 = [h_{1,1} \ h_{1,2} \ h_{4,1} \ h_{4,5} \ h_{7,2} \ h_{7,5}]$ 
19:    Remove interference signals in  $\mathbb{B}_1$  from  $\mathbb{X}_1$ 
20:     $\mathcal{J}_i = [] \ \mathbb{Q}_i = []$  for  $i = 1, 2$ 
21:  END FOR

```

$$\mathbb{A} = \begin{pmatrix} h_{1,1} & h_{1,2} & h_{4,1} & h_{4,5} & h_{7,2} & h_{7,5} \\ h_{1,1} & h_{1,2} & h_{3,1} & h_{3,4} & h_{6,2} & h_{6,4} \\ h_{1,1} & h_{1,2} & h_{2,1} & h_{2,3} & h_{5,2} & h_{5,3} \\ h_{2,1} & h_{2,3} & h_{4,1} & h_{4,5} & h_{9,3} & h_{9,5} \\ h_{2,1} & h_{2,3} & h_{3,1} & h_{3,4} & h_{8,3} & h_{8,4} \\ h_{3,1} & h_{3,4} & h_{4,1} & h_{4,5} & h_{10,4} & h_{10,5} \\ h_{5,2} & h_{5,3} & h_{7,2} & h_{7,5} & h_{9,3} & h_{9,5} \\ h_{5,2} & h_{5,3} & h_{6,2} & h_{6,4} & h_{8,3} & h_{8,4} \\ h_{6,2} & h_{6,4} & h_{7,2} & h_{7,5} & h_{10,4} & h_{10,4} \\ h_{8,3} & h_{8,4} & h_{10,4} & h_{10,5} & h_{9,3} & h_{9,5} \end{pmatrix},$$

$$\mathbb{B} = \begin{pmatrix} \mathbf{X}_1^{2,3} & \mathbf{X}_2^{2,3} & \mathbf{X}_5^{3,4} \\ \mathbf{X}_1^{2,4} & \mathbf{X}_2^{2,4} & \mathbf{X}_4^{3,4} \\ \mathbf{X}_1^{3,4} & \mathbf{X}_2^{3,4} & \mathbf{X}_3^{3,4} \\ \mathbf{X}_1^{1,3} & \mathbf{X}_3^{2,3} & \mathbf{X}_5^{2,4} \\ \mathbf{X}_1^{1,4} & \mathbf{X}_3^{2,4} & \mathbf{X}_4^{2,4} \\ \mathbf{X}_1^{1,2} & \mathbf{X}_4^{2,3} & \mathbf{X}_5^{2,3} \\ \mathbf{X}_2^{1,3} & \mathbf{X}_3^{1,3} & \mathbf{X}_5^{1,4} \\ \mathbf{X}_2^{1,4} & \mathbf{X}_3^{1,4} & \mathbf{X}_4^{1,4} \\ \mathbf{X}_2^{1,2} & \mathbf{X}_4^{1,3} & \mathbf{X}_5^{1,3} \\ \mathbf{X}_4^{1,2} & \mathbf{X}_3^{1,2} & \mathbf{X}_5^{1,2} \end{pmatrix}, \quad \mathbb{C} = \begin{pmatrix} \text{UE}_1 & \text{UE}_4 & \text{UE}_7 \\ \text{UE}_1 & \text{UE}_3 & \text{UE}_6 \\ \text{UE}_1 & \text{UE}_2 & \text{UE}_5 \\ \text{UE}_2 & \text{UE}_4 & \text{UE}_9 \\ \text{UE}_2 & \text{UE}_3 & \text{UE}_8 \\ \text{UE}_3 & \text{UE}_4 & \text{UE}_{10} \\ \text{UE}_5 & \text{UE}_7 & \text{UE}_9 \\ \text{UE}_5 & \text{UE}_6 & \text{UE}_8 \\ \text{UE}_6 & \text{UE}_7 & \text{UE}_{10} \\ \text{UE}_8 & \text{UE}_{10} & \text{UE}_9 \end{pmatrix}.$$

Then, for each signal in \mathbb{B}_g , we construct a constellation that is scaled by the monomial set $\mathcal{G}(\mathbb{A}_g)$, i.e, the signals $\mathbf{X}_2^{2,4}$ in \mathbb{B}_2 use the monomials in $\mathcal{G}(\mathbb{A}_2)$, resulting in the signal constellation $\sum_{v \in \mathcal{G}(\mathbb{A}_g)} v\mathbb{Z}_Q$.

Focusing on Example 1, we want to assess whether the interfering signals have been aligned, and whether the requested subfiles arrive with independent channel coefficients, the decodability is guaranteed. Starting with u_1 , the received constellation corresponding to the desired signals $\mathbf{X}_1^{1,2}$, $\mathbf{X}_1^{1,3}$, $\mathbf{X}_1^{1,4}$, $\mathbf{X}_2^{1,2}$, $\mathbf{X}_2^{1,3}$ and $\mathbf{X}_2^{1,4}$:

$$\begin{aligned} C_D &= h_{1,1} \sum_{v \in \mathcal{G}(\mathbb{A}_6)} v\mathbb{Z}_Q + h_{1,1} \sum_{v \in \mathcal{G}(\mathbb{A}_4)} v\mathbb{Z}_Q + h_{1,1} \sum_{v \in \mathcal{G}(\mathbb{A}_5)} v\mathbb{Z}_Q \\ &+ h_{1,2} \sum_{v \in \mathcal{G}(\mathbb{A}_9)} v\mathbb{Z}_Q + h_{1,2} \sum_{v \in \mathcal{G}(\mathbb{A}_7)} v\mathbb{Z}_Q + h_{1,2} \sum_{v \in \mathcal{G}(\mathbb{A}_8)} v\mathbb{Z}_Q. \end{aligned} \quad (16)$$

The received constellation for the interfering signals $\mathbf{X}_1^{2,3}$, $\mathbf{X}_2^{2,3}$, $\mathbf{X}_1^{2,4}$, $\mathbf{X}_2^{2,4}$, $\mathbf{X}_2^{3,4}$ and $\mathbf{X}_2^{3,4}$ is

$$\begin{aligned} C_I &= h_{1,1} \sum_{v \in \mathcal{G}(\mathbb{A}_1)} v\mathbb{Z}_Q + h_{1,2} \sum_{v \in \mathcal{G}(\mathbb{A}_1)} v\mathbb{Z}_Q + h_{1,1} \sum_{v \in \mathcal{G}(\mathbb{A}_2)} v\mathbb{Z}_Q \\ &+ h_{1,2} \sum_{v \in \mathcal{G}(\mathbb{A}_2)} v\mathbb{Z}_Q + h_{1,1} \sum_{v \in \mathcal{G}(\mathbb{A}_3)} v\mathbb{Z}_Q + h_{1,2} \sum_{v \in \mathcal{G}(\mathbb{A}_3)} v\mathbb{Z}_Q. \end{aligned} \quad (17)$$

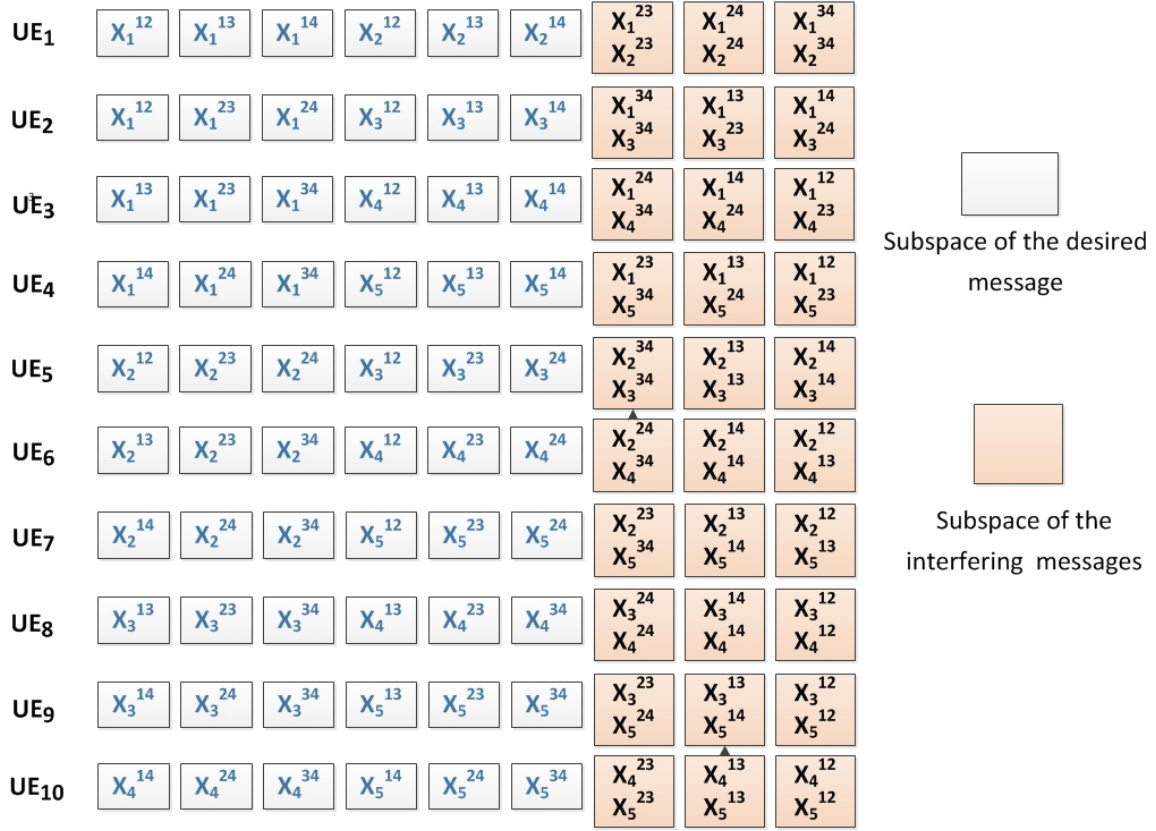


Fig. 3: The signal space for UEs in Example 1 after applying real IA.

Eqn. (17) proves that every two interfering signals, one from each EN, i.e., the first two terms in Eqn. (17), have collapsed into the same sub-space. Also, since the monomials $\mathcal{G}(\mathbb{A}_1)$, $\mathcal{G}(\mathbb{A}_2)$ and $\mathcal{G}(\mathbb{A}_3)$ do not overlap and linear independence is obtained, the interfering signals will align in $I = 3$ different sub-spaces. We can also see in (16) that the monomials corresponding to the intended messages do not align, and rational independence is guaranteed (with high probability), and the desired signals will be received over 6 different subspaces. Since the monomials form different constellations, C_D and C_I , whose terms are functions of different channel coefficients, we can assert that these monomials do not overlap. Hence, we can claim that IA is achieved. Our scheme guarantees that the desired signals at each user will be received in $r \binom{L-1}{t_E}$ different subspaces, and each r interfering signals will be aligned into the same subspace, i.e., one from each EN, resulting in a total of $I = \binom{L}{t_E+1} - \binom{L-1}{t_E}$ interference subspaces. The signal space for UEs in Example 1 after applying real IA is given in Fig. 3.

When $t_E = L - 1$, the number of interference signals at each user is $I = 0$. Hence, we just transmit the constellation points corresponding to each signal. We are sure that the decodability

is guaranteed since all channel coefficients are i.i.d. according to a continuous distribution.

UE_k utilizes its cache content Z_k to extract $f_{k,\mathcal{T}}^i$, for $i \in \mathcal{N}_k$ and $\text{Index}(i, k) \notin \mathcal{T}$. Therefore, UE_k reconstructs f_k^i and decodes its requested file W_k . In Example 1, UE₁ utilizes its memory Z_1 in TABLE I to extract $f_{1,\mathcal{T}}^i$, for $i = 1, 2$, and $\mathcal{T} = \{2, 3, 4\}$. Hence, UE₁ reconstructs f_1^1 and f_1^2 , and decodes its requested file W_1 ; and similarly for the remaining UEs. Thus, the edge NDT from ENs to the UEs is equal to $\delta_E(\frac{1}{4}, 0, \rho) = \frac{9}{8}$, while the total NDT is $\delta(\frac{1}{4}, 0, \rho) = \frac{3}{4\rho} + \frac{9}{8}$. In the general case, the NDT from the ENs to the UEs by using the MDS-IA scheme is given by

$$\delta_E(\mu_R, 0, \rho) = \frac{\binom{L-1}{t_E}(r-1) + \binom{L}{t_E+1}}{r \binom{L}{t_E}} = \frac{L-t_E}{r} \left(\frac{r-1}{L} + \frac{1}{t_E+1} \right). \quad (18)$$

Together with the fronthaul NDT in (13), we obtain the end-to-end NDT in Theorem 1. NDT achieved by the MDS-IA for various system parameters is presented in Section VII.

B. MDS-IA Scheme with Cache Enabled ENs

IN the MDS-IA scheme, when $\mu_T \geq \frac{1}{r}$, i.e., each EN_i, $i \in [K]$, can cache the encoded subfile f_n^i , $\forall n$, and the users' requests can be satisfied without the participation of the cloud server in the delivery phase, i.e., $\rho = 0$. In this case each EN_i, $i \in [K]$, can act as a server for its connected UEs, and we can use the same placement scheme in Section IV-A for the UEs, and the same delivery scheme in Section IV-A- Step 2, given that the coded multicast messages in (11) can now be generated locally at the ENs. Then, end-to-end achievable NDT is given by

$$\delta_{\text{MDS-IA}}(\mu_R, \mu_T, \rho) = \frac{L-t_E}{r} \left[\frac{r-1}{L} + \frac{1}{t_E+1} \right] \quad (19)$$

1) **Cache Placement Phase:** In the following, we extend the proposed scheme to the case with $0 \leq \mu_T < 1/r$. We use a similar cache placement scheme to the one in [21]. We form the coded chunks f_n^i as in Section IV-A. Then, the server divides each chunk into two parts, $f_n^{i,1}$ and $f_n^{i,2}$, with sizes $\mu_T F$ and $(\frac{1}{r} - \mu_T)F$, respectively. The cloud server places $f_n^{i,1}$, $\forall n$, in the cache memory of EN_i, where the total size of the cached pieces is $\mu_T N F$, satisfying the cache memory constraint with equality. The UE cache placement scheme is the same as in Section IV-A. At the end of the placement phase, each user stores $N r \binom{L-1}{t_E-1}$ pieces from each set of the encoded chunks, which sum up to $\mu_R N F$, satisfying the UE cache memory constraint with equality.

2) **Delivery Phase:** Delivery phase is divided into two parts. In the first part, the cloud server delivers the subfiles in

$$\{f_{d_k, \mathcal{T}}^{i,2} : k \notin \mathcal{T}, \mathcal{T} \subseteq [L], |\mathcal{T}| = t_E\} \quad (20)$$

to UE_k , i.e., the subfiles of $f_{d_k}^{i,2}$ that have not been already stored in the cache memories of UE_k and EN_i . The total number of such subfiles is $\binom{L}{t_E} - \binom{L-1}{t_E-1}$. For these, we use the same delivery scheme in Section IV-A-2. The achievable NDT is given by

$$\delta_{\text{MDS-IA}}(\mu_R, \mu_T, \rho) = \left(\frac{1}{r} - \mu_T\right) (L - t_E) \left[\frac{r-1}{L} + \frac{1}{t_E+1} \left(1 + \frac{1}{\rho}\right) \right], \quad (21)$$

where the factor $\left(\frac{1}{r} - \mu_T\right)$ is due to the reduction in the size of the coded multicast message from the cloud server to the ENs thanks to the already cached contents in EN caches.

In the second part, ENs deliver the subfiles in

$$\{f_{d_k, \mathcal{T}}^{i,1} : k \notin \mathcal{T}, \mathcal{T} \subseteq [L], |\mathcal{T}| = t_E\} \quad (22)$$

to UE_k , i.e., the subfiles of file $f_{d_k}^{i,1}$ which have been cached by EN_i but not by UE_k . The total number of such subfiles is $\binom{L}{t_E} - \binom{L-1}{t_E-1}$. For this case, we use the delivery scheme from the ENs to the UEs presented in Section IV-A-2, where the coded multicaste message

$$\mathbf{X}_{i,1}^S \triangleq \bigoplus_{k:k \in \mathcal{K}_i, \text{Index}(i,k) \in \mathcal{S}} f_{d_k, \mathcal{S} \setminus \text{Index}(i,k)}^{i,1} \quad (23)$$

will be generated locally at EN_i , where $|\mathbf{X}_{i,1}^S| = \frac{\mu_T F}{\binom{L}{t_E}}$ bits. Accordingly, the fronthaul NDT from the cloud server to the ENs is zero. By following the same approach of Section IV-A Step 2, the achievable NDT from the ENs to the UEs is given by

$$\delta_E(\mu_R, \mu_T, \rho) = \mu_T \frac{\binom{L-1}{t_E}(r-1) + \binom{L}{t_E+1}}{\binom{L}{t_E}} = \mu_T (L - t_E) \left(\frac{r-1}{L} + \frac{1}{t_E+1} \right). \quad (24)$$

Together with the NDT in (21), we obtain the end-to-end NDT as given in Theorem 1.

V. SOFT-TRANSFER SCHEME

As in the MDS-IA scheme it is easier and more intuitive to first introduce a RACN architecture without cache memories at the ENs. Generalization to cache-enabled ENs will follow easily from this initial scheme.

A. Soft-Transfer Scheme with out Cache Memories at the ENs

Here, we present a centralized caching scheme for with receiver connectivity r , and $t_U \in [K]$ when there is no cache memory at the ENs. The soft-transfer of channel input symbols over fronthaul links is proposed in [32], where the cloud server implements ZF-beamforming and quantizes the encoded signal to be transmitted to each EN. Therefore, the fronthaul NDT is given by

$$\delta_{F\text{-soft}}(\mu_R, \mu_T, \rho) = \left(1 - \frac{t_U}{K}\right) \frac{K}{H\rho}, \quad (25)$$

while the total NDT can be expressed as

$$\delta_{\text{soft}}(\mu_R, \mu_T, \rho) = \delta_{E\text{-Ideal}} + \delta_{F\text{-soft}}, \quad (26)$$

where $\delta_{E\text{-Ideal}}$ is the achievable edge NDT in an ideal system in which the ENs can acts as one big multi-antenna transmitter. This is equivalent to assuming that the whole library \mathcal{W} can be cached at all the ENs; and hence, full cooperation among the ENs is possible for any user demand vector. We will provide a coding scheme that uses ZF for this ideal system to provide a general expression for $\delta_{E\text{-Ideal}}$.

1) **Cache Placement Phase:** For any file W_n in the library, $n \in [N]$, we partition it into $\binom{K}{t_U}$ equal-size subfiles, each of which is denoted by $W_{n,\mathcal{T}}$, where $\mathcal{T} \subseteq [K]$, $|\mathcal{T}| = t_U$. The subfiles $W_{n,\mathcal{T}}, \forall n$, are stored in the cache memory of UE_k if $k \in \mathcal{T}$. At the end of the placement phase, each user stores $N \binom{K-1}{t_U-1}$ subfiles, each of size $\frac{F}{\binom{K}{t_U}}$ bits, which sum up to MF bits, satisfying the cache capacity constraint with equality.

Example 2. Consider the 4×6 RACN architecture with $H = 4$, $K = N = 6$, $r = 2$, $\mu_T = 0$ bits and $L = 3$. For $t_U = 2$, file $W_n, \forall n \in [N]$, is divided into $\binom{6}{2} = 15$ disjoint subfiles $W_{n,\mathcal{T}}$, where $\mathcal{T} \subseteq [K]$ and $|\mathcal{T}| = t_U = 2$. The size of each subfile is $\frac{F}{15}$ bits. Cache contents of each user are listed in TABLE IV. Observe that each user stores $6 \binom{5}{1} = 30$ subfiles, each of size $\frac{F}{15}$ bits, which sum up to $2F$ bits, satisfying the memory constraint with equality.

2) **Delivery Phase:** Let W_{d_k} denote the request of user $\text{UE}_k, k \in [K]$. Then, the ENs need to deliver the subfiles in

$$\{W_{d_k,\mathcal{T}} : k \notin \mathcal{T}, \mathcal{T} \subseteq [K], |\mathcal{T}| = t_U\} \quad (27)$$

to UE_k , i.e., the subfiles of file W_{d_k} that have not been stored in the cache of UE_k . The total number of such subfiles is $\binom{K}{t_U} - \binom{K-1}{t_U-1}$.

User	UE ₁	UE ₂	UE ₃	UE ₄	UE ₅	UE ₆
Cache	$W_{n,12}$	$W_{n,12}$	$W_{n,13}$	$W_{n,14}$	$W_{n,15}$	$W_{n,16}$
	$W_{n,13}$	$W_{n,23}$	$W_{n,23}$	$W_{n,24}$	$W_{n,25}$	$W_{n,26}$
	$W_{n,14}$	$W_{n,24}$	$W_{n,34}$	$W_{n,34}$	$W_{n,35}$	$W_{n,36}$
	$W_{n,15}$	$W_{n,25}$	$W_{n,35}$	$W_{n,45}$	$W_{n,45}$	$W_{n,46}$
	$W_{n,16}$	$W_{n,26}$	$W_{n,36}$	$W_{n,46}$	$W_{n,56}$	$W_{n,56}$

TABLE IV: Cache contents after the placement phase for the RACN scenario considered in Example 2, where $K = N = 6$, $r = 2$, $L = 3$, $t_U = 2$ and $\mu_R = \frac{1}{3}$.

User	UE ₁		UE ₂		UE ₃		UE ₄		UE ₅		UE ₆	
Missing subfiles	$W_{1,23}$	$W_{1,35}$	$W_{2,13}$	$W_{2,35}$	$W_{3,12}$	$W_{3,25}$	$W_{4,12}$	$W_{4,25}$	$W_{5,12}$	$W_{5,24}$	$W_{6,12}$	$W_{6,24}$
	$W_{1,24}$	$W_{1,36}$	$W_{2,14}$	$W_{2,36}$	$W_{3,14}$	$W_{3,26}$	$W_{4,13}$	$W_{4,26}$	$W_{5,13}$	$W_{5,26}$	$W_{6,13}$	$W_{6,25}$
	$W_{1,25}$	$W_{1,45}$	$W_{2,15}$	$W_{2,45}$	$W_{3,15}$	$W_{3,45}$	$W_{4,15}$	$W_{4,35}$	$W_{5,14}$	$W_{5,34}$	$W_{6,14}$	$W_{6,34}$
	$W_{1,26}$	$W_{1,46}$	$W_{2,16}$	$W_{2,46}$	$W_{3,16}$	$W_{3,46}$	$W_{4,16}$	$W_{4,36}$	$W_{5,16}$	$W_{5,36}$	$W_{6,15}$	$W_{6,35}$
	$W_{1,34}$	$W_{1,56}$	$W_{2,34}$	$W_{2,56}$	$W_{3,24}$	$W_{3,56}$	$W_{4,23}$	$W_{4,56}$	$W_{5,23}$	$W_{5,46}$	$W_{6,23}$	$W_{6,45}$

TABLE V: Missing subfiles for each user's request in Example 2. These subfiles must be delivered to the corresponding user within the delivery phase.

For Example 2, assuming, without loss of generality, that UE_{*k*} requests W_k , the missing subfiles of each user request, to be delivered in the delivery phase, are listed in TABLE V.

We first describe the delivery phase when $K - H \leq t_U \leq K - 1$. We will later consider the case $t_U < K - H$ separately. Note that, when $t_U = K$ the achievable NDT is equal to zero since each user can cache all the N files.

Case 1 ($K - H \leq t_U \leq K - 1$): We introduce an alternative representation for each subfile in (35), which will denote the UEs at which each of these subfiles will be zero-forced. In particular, we will denote subfile $W_{d_k, \mathcal{T}}$ by $W_{d_k, \mathcal{T}, \pi}$, where $\pi \subseteq [K] \setminus (\{k\} \cup \mathcal{T})$, $|\pi| = K - (t_U + 1)$, denotes the set of receivers at which this subfile will be zero-forced. The total number of subfiles intended for UE_{*k*} is $\binom{K}{t_U} - \binom{K-1}{t_U-1}$ subfiles. TABLE VI shows this alternative representation for the missing subfiles for each user in Example 2.

All the ENs will transmit $W_{d_k, \mathcal{T}, \pi}$ by using the beamforming vector $\mathbf{v}_\pi \in \mathbb{R}^H$ to zero-force this subfile at the UEs in π . We define the matrix \mathbf{H}_π with dimensions $K - (t_U + 1) \times H$ to be the channel matrix from the ENs to the UEs in π and the set of ENs \mathcal{E} . The beamforming

User	UE ₁		UE ₂		UE ₃		UE ₄		UE ₅		UE ₆	
Missing subfiles	$W_{1,23,456}$	$W_{1,35,246}$	$W_{2,13,456}$	$W_{2,35,146}$	$W_{3,12,456}$	$W_{3,25,146}$	$W_{4,12,356}$	$W_{4,25,136}$	$W_{5,12,346}$	$W_{5,24,136}$	$W_{6,12,345}$	$W_{6,24,135}$
	$W_{1,24,356}$	$W_{1,36,245}$	$W_{2,14,356}$	$W_{2,36,145}$	$W_{3,14,256}$	$W_{3,26,145}$	$W_{4,13,256}$	$W_{4,26,135}$	$W_{5,13,246}$	$W_{5,26,134}$	$W_{6,13,245}$	$W_{6,25,134}$
	$W_{1,25,346}$	$W_{1,45,236}$	$W_{2,15,346}$	$W_{2,45,136}$	$W_{3,15,246}$	$W_{3,45,126}$	$W_{4,15,236}$	$W_{4,35,126}$	$W_{5,14,236}$	$W_{5,34,126}$	$W_{6,14,235}$	$W_{6,34,125}$
	$W_{1,26,345}$	$W_{1,46,235}$	$W_{2,16,345}$	$W_{2,46,135}$	$W_{3,16,245}$	$W_{3,46,125}$	$W_{4,16,235}$	$W_{4,36,125}$	$W_{5,16,234}$	$W_{5,36,124}$	$W_{6,15,234}$	$W_{6,35,124}$
	$W_{1,34,256}$	$W_{1,56,234}$	$W_{2,34,156}$	$W_{2,56,134}$	$W_{3,24,156}$	$W_{3,56,124}$	$W_{4,23,156}$	$W_{4,56,123}$	$W_{5,23,146}$	$W_{5,46,123}$	$W_{6,23,145}$	$W_{6,45,123}$

TABLE VI: The alternative representation of the missing subfiles of each user in Example 2, including the UEs at which each subfile will be zero-forced at.

vector \mathbf{v}_π is designed as follows:

$$\mathbf{v}_\pi = \sum_{i=1}^D \mathbf{v}_i, \quad (28)$$

where $D = H - K + (t_U + 1)$ is the size of the null space of the matrix \mathbf{H}_π , while \mathbf{v}_i is the i th basis vector of this null space. The null space of matrix \mathbf{H}_π with $1 \leq |\pi| \leq H - 1$ always has a non-zero element since $D \geq 1$. Hence, the subfile $W_{d_k, \mathcal{T}, \pi}$ for any $\pi \geq 1$ can be always zero-forced at the UEs in π . In Example 2, the size of the null space is $D = 1$.

In each step of the delivery phase, we transmit one subfile from each requested file, which means that we will have $\binom{K}{t_U} - \binom{K-1}{t_U-1}$ steps in total. The transmitted set of subfiles at each step will be decoded by their intended receivers without any interference since each subfile $W_{d_k, \mathcal{T}, \pi}$ in this set is already cached at $|\mathcal{T}| = t_U$ UEs, $\mathcal{T} \subseteq \mathcal{U}$, and will be zero-forced at $|\pi| = K - (t_U + 1)$ other UEs, $\pi \subseteq \mathcal{U}$. Since $\mathcal{T} \cap \pi = \emptyset$ and $|\mathcal{T}| + |\pi| = |\mathcal{U}| - 1$, each subfile will not cause any interference at the $|K| - 1$ undesired UEs. Hence, the edge NDT of the ideal system is given by

$$\delta_{E\text{-Ideal}}(\mu_R, \mu_T, \rho) = \frac{K - t_U}{K}. \quad (29)$$

The end-to-end achievable NDT for the soft-transfer scheme is given by

$$\delta_{\text{soft}}(\mu_R, \mu_T, \rho) = (K - t_U) \left(\frac{1}{K} + \frac{1}{H\rho} \right). \quad (30)$$

In Example 2, the delivery phase of the soft-transfer scheme consists of $\binom{6}{2} - \binom{5}{1} = 10$ steps. At each step all the ENs will cooperate to transmit $K = 6$ subfiles, one for each user, by acting as one transmitter with 4 antennas according to the ideal system assumption. In Fig. 4, we show one step of the delivery phase given that all the ENs cooperate to deliver the missing subfiles, i.e., the ideal system as discussed earlier. In this figure, we can see that each user will be able to decode its desired subfile without any interference, as the undesired subfiles are either cached or zero-forced at this user. The edge NDT of this ideal system is $\delta_{E\text{-Ideal}} = \frac{2}{3}$, while the achievable

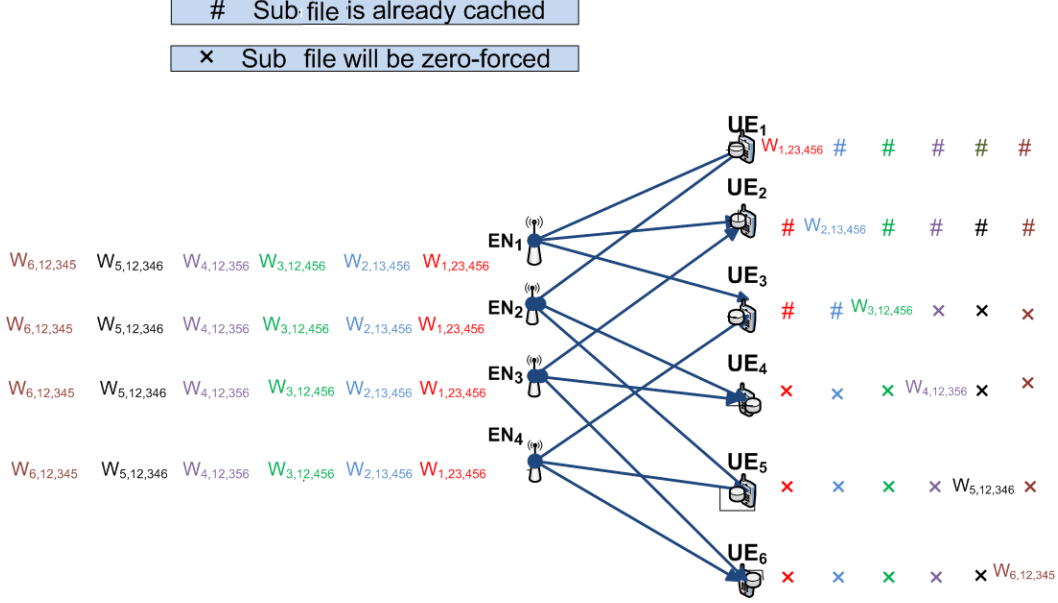


Fig. 4: One step of the delivery phase for the RACN architecture in Example 2 with receiver connectivity $r = 2$, where $H = 4$ ENs serve $K = 6$ UEs.

end-to-end NDT for the soft-transfer scheme is $\delta_{\text{soft}}(\frac{1}{3}, 0, \rho) = \frac{2}{3} + \frac{1}{\rho}$.

Case 2 ($t_U < K - H$): In this case each subfile $W_{d_k, \mathcal{T}}$ in (35) is partitioned into $\binom{K-(t_U+1)}{H-1}$ disjoint chunks of equal size, denoted by

$$W_{d_k, \mathcal{T}} = \{W_{d_k, \mathcal{T}, \pi, \pi'} : \pi \subseteq [K] \setminus (\{k\} \cup \mathcal{T}), |\pi| = H - 1, \quad (31)$$

$$\pi' \subseteq [K] \setminus (\{k\} \cup \mathcal{T} \cup \pi)\},$$

where π , $|\pi| = H - 1$, is the set of receivers at which this chunk will be zero-forced, while π' , $|\pi'| = K - (H + t_U)$, is the set of receivers at which this chunk will cause interference, i.e., the set of receivers at which this chunk is neither cached nor zero-forced. The total number of chunks intended for user UE_k is $\left(\binom{K}{t_U} - \binom{K-1}{t_U-1}\right) \binom{K-(t_U+1)}{H-1}$, while the size of each chunk is $|W_{d_k, \mathcal{T}, \pi, \pi'}| = \frac{F}{\binom{K}{t_U} \binom{K-(t_U+1)}{H-1}}$ bits.

All the ENs \mathcal{E} transmit $W_{d_k, \mathcal{T}, \pi, \pi'}$ by using the beamforming vector $\mathbf{v}_\pi \in \mathbb{R}^H$ to zero-force this chunk at the UEs in set π . The matrix \mathbf{H}_π for this case is of dimensions $(H - 1) \times H$. The beamforming vector \mathbf{v}_π is designed as follow $\mathbf{v}_\pi = \text{Null}\{\mathbf{H}_\pi\}$, where $\text{Null}\{\mathbf{H}_\pi\}$ is the null space of matrix \mathbf{H}_π . The null space always exist, and its size is 1.

At each step of delivery phase, we transmit the set of chunks that have the same π' and belong to different requested files, i.e., we transmit at most one chunk from each requested file at the

same time. In other words, in each step we transmit the set of chunks that belong to different requested files, but cause interference at the same set of receivers. The size of each transmitted set per step is $H + t_U$. This is because, the chunks that have the same π' do not belong to the set of requested files $\{W_{d_k} : k \in \pi'\}$, with size $K - (H + t_U)$, and will only belong to the one of the remaining $(H + t_U)$ requested files, denoted by the set $\mathcal{R} = \{W_{d_k} : k \notin \pi'\}$, while we only transmit the chunks that belong to different requested files at the same time.

Each user is interested in $\left(\binom{K}{t_U} - \binom{K-1}{t_U-1}\right) \binom{K-(t_U+1)}{H-1}$ chunks, while the total number of requested files is K , and in every step we transmit only $(H + t_U)$ chunks. Hence, the total number of steps is given by

$$\frac{\left(\binom{K}{t_U} - \binom{K-1}{t_U-1}\right) \binom{K-(t_U+1)}{H-1} K}{H + t_U}. \quad (32)$$

We denote the set of UEs interested in the transmitted $(H + t_U)$ chunks that have the same π' and belong to different requested files by $\mathcal{U}_{\pi'} = \{\mathcal{U} \setminus \pi'\}$, where $|\mathcal{U}_{\pi'}| = H + t_U$. For chunk $W_{d_k, \mathcal{T}, \pi, \pi'}$ requested by user $UE_k \in \mathcal{U}_{\pi'}$, we have $(\mathcal{T} \cup \pi \cup \pi') \subseteq \mathcal{U}$; and hence, $(\mathcal{T} \cup \pi) \subseteq \mathcal{U}_{\pi'}$. The set of transmitted chunks will be decoded by the UEs in set $\mathcal{U}_{\pi'}$ without interference since each chunk $W_{d_k, \mathcal{T}, \pi, \pi'}$ in this set is already cached at $|\mathcal{T}| = t_U$ UEs, where $\mathcal{T} \subseteq \mathcal{U}_{\pi'}$, and will be zero-forced at $|\pi| = H - 1$ UEs, $\pi \subseteq \mathcal{U}_{\pi'}$. Since $\mathcal{T} \cap \pi = \emptyset$ and $|\mathcal{T}| + |\pi| = |\mathcal{U}_{\pi'}| - 1$, which means that each chunk will not cause any interference at the $|\mathcal{U}_{\pi'}| - 1$ undesired UEs in set $\mathcal{U}_{\pi'}$. Hence, each user in this set $\mathcal{U}_{\pi'}$ can decode its desired chunk, the edge NDT of the ideal system in this case is given by

$$\delta_{E\text{-Ideal}}(\mu_R, \mu_T, \rho) = \frac{K - t_U}{K} \frac{K}{H + t_U}. \quad (33)$$

The achievable end-to-end NDT by using the soft-transfer scheme in case 2 is given by

$$\delta_{\text{soft}}(\mu_R, \mu_T, \rho) = (K - t_U) \left(\frac{1}{H + t_U} + \frac{1}{H\rho} \right). \quad (34)$$

B. Soft-Transfer Scheme with Cache Enabled ENs

1) **Cache Placement Phase:** The cloud server divides each file W_n in the library, $n \in [N]$, into two parts W_n^1 and W_n^2 with sizes $\mu_T F$ bits and $(1 - \mu_T)F$ bits, respectively. At first, the cloud server places W_n^1 , $n \in [N]$, in the cache memory of all the ENs. Then, the UEs apply the placement scheme in Section V-A-1 on the two sets W_n^1 and W_n^2 , $\forall n$. At the end of the placement phase, each user stores $N \binom{K-1}{t_U-1}$ pieces from each set, each piece $W_{n, \mathcal{T}}^1$, where

$\mathcal{T} \subseteq [K]$, $|\mathcal{T}| = t_U$, has a size $\frac{\mu_T F}{\binom{K}{t_U}}$ bits while the size of each piece $W_{n,\mathcal{T}}^2$, where $\mathcal{T} \subseteq [K]$, $|\mathcal{T}| = t_U$, is $\frac{(1-\mu_T)F}{\binom{K}{t_U}}$, which sum up to $\mu_R N F$ bits, satisfying the memory constraint with equality.

2) **Delivery Phase:** In the first part, the cloud server needs to deliver the subfiles

$$\{W_{d_k,\mathcal{T}}^2 : k \notin \mathcal{T}, \mathcal{T} \subseteq [K], |\mathcal{T}| = t_U\} \quad (35)$$

to UE_k , i.e., the subfiles of file $W_{d_k}^2$ which have not been already stored in the cache of UE_k . The total number of such subfiles is $\binom{K}{t_U} - \binom{K-1}{t_U-1}$. For this case, we use the same delivery phase of the soft-transfer scheme presented in Section V-A-2. The achievable NDT is given by

$$\delta_{\text{soft}}(\mu_R, \mu_T, \rho) = (1 - \mu_T)(K - t_U) \left[\frac{1}{\min\{H + t_U, K\}} + \frac{1}{H\rho} \right]. \quad (36)$$

In the second part of the delivery phase, the ENs deliver the subfiles in

$$\{W_{d_k,\mathcal{T}}^1 : k \notin \mathcal{T}, \mathcal{T} \subseteq [K], |\mathcal{T}| = t_U\} \quad (37)$$

to UE_k , i.e., the subfiles of file $W_{d_k}^1$ which have been stored in the cache memory of the ENs and have not been already stored in the cache of UE_k . The total number of such subfiles is $\binom{K}{t_U} - \binom{K-1}{t_U-1}$. For this case, we can use the same delivery scheme from the ENs to the UEs which is based on ZF and presented in Section V-A-2, since each EN_i , $i \in [H]$, caches all the requested subfiles in (37). According to that, the end-to-end achievable NDT for the this case is given by

$$\delta_{\text{soft}}(\mu_R, \mu_T, \rho) = \mu_T(K - t_U) \left[\frac{1}{\min\{H + t_U, K\}} \right]. \quad (38)$$

Together with the achievable NDT in (36), we obtain the end-to-end NDT in Theorem 2.

VI. ZERO-FORCING (ZF) SCHEME

In this section, we present a centralized coded caching scheme for the same RACN architecture with receiver connectivity r with $\mu_R + \mu_T \geq 1$ and $t_R = \frac{(\mu_R + \mu_T - 1)K}{\mu_T}$.

A. Placement Phase

The cloud server divides each file W_n in the library, $n \in [N]$, into two parts W_n^1 and W_n^2 with sizes $\mu_T F$ bits and $(1 - \mu_T)F$ bits, respectively. First, the cloud server places W_n^1 , $\forall n$, in the cache memory of all the ENs. After that, each UE_k , $k \in [K]$, cache the whole set $\{W_n^2, n \in [N]\}$.

For any file W_n^1 , $n \in [N]$, we partition it into $\binom{K}{t_R}$ equal-size subfiles, each of which is denoted by $W_{n,\mathcal{T}}^1$, where $\mathcal{T} \subseteq [K]$, $|\mathcal{T}| = t_R$. The subfiles $W_{n,\mathcal{T}}^1$, $\forall n$, are stored in the cache memory of UE $_k$ if $k \in \mathcal{T}$. At the end of the placement phase, each user stores $N \binom{K-1}{t_R-1}$ subfiles, each of size $\frac{\mu_T F}{\binom{K}{t_R}}$ bits, from the set of cached subfiles at the ENs and stores the set $\{W_n^2, n \in [N]\}$, that has a size of $(1 - \mu_T)NF$ bits, which sum up to $\mu_R NF$ bits, satisfying the cache capacity constraint with equality.

B. Delivery Phase

The ENs need to deliver the subfiles in

$$\{W_{d_k,\mathcal{T}}^1 : k \notin \mathcal{T}, \mathcal{T} \subseteq [K], |\mathcal{T}| = t_R\} \quad (39)$$

to UE $_k$, i.e., the subfiles of file $W_{d_k}^1$ which have been stored in the cache memory of the ENs and have not been already stored in the cache of UE $_k$. The total number of such subfiles is $\binom{K}{t_R} - \binom{K-1}{t_R-1}$. For this case, we can use ZF-based delivery scheme in Section V-A-2, since each EN $_i$, $i \in [H]$ caches all the requested subfiles in (39) and hence the ENs can act as one big multi-antenna transmitter where full cooperation is possible among the ENs for any user demand vector. This result in the end-to-end NDT in Theorem 3.

VII. NUMERICAL RESULTS

In this section we compare the end-to-end latency achieved by the three proposed schemes. The NDTs achieved by the MDS-IA, soft-transfer and zero-frcing schemes for three different fronthaul multiplexing gains are plotted in Fig. 5. We observe that the end-to-end NDT decreases with increasing ρ and the NDT in Fig. 5a is mainly dominated by the edge NDT for the soft-transfer and the MDS-IA schemes. We also observe that, caches at the ENs allow reducing the end-to-end NDT as expected, but the amount of reduction becomes negligible as ρ increases, since the files can now be delivered efficiently over the fronthaul links. We also observe that the best performance among the three schemes depends highly on ρ and the total cache size of the ENs and the UEs. In Fig. 5a and Fig. 5c with $\rho = 0.05$ and $\rho = 0.2353$, respectively, when the total cache size of one UE and one EN is not sufficient to store the entire library, i.e., $\mu_R < 0.7$, the MDS-IA scheme performs better than the soft-transfer scheme for almost all cache capacity values, while we observe in Fig. 5b that the soft-transfer scheme outperforms MDS-IA as the multiplexing gain increases, i.e., $\rho = 20$. This is mainly because the edge latency of the soft

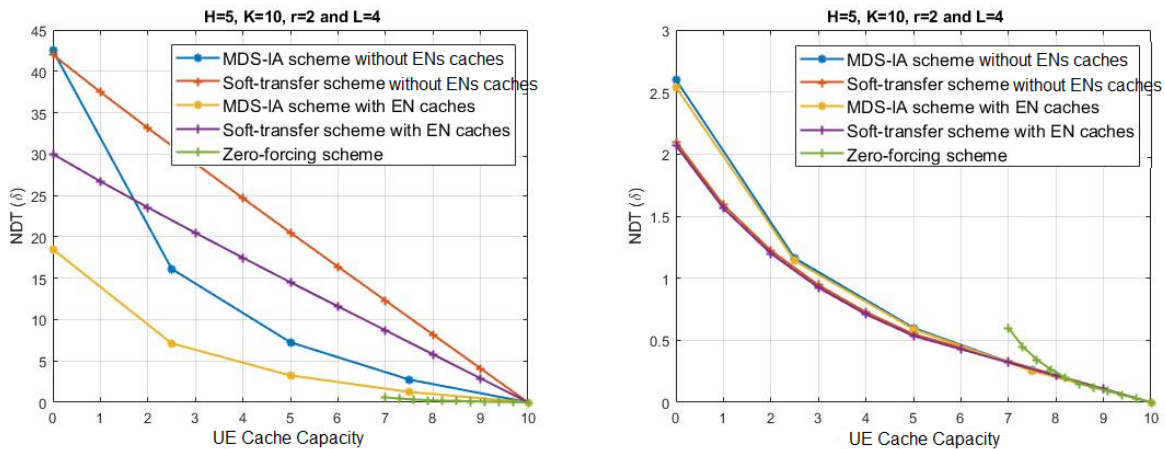
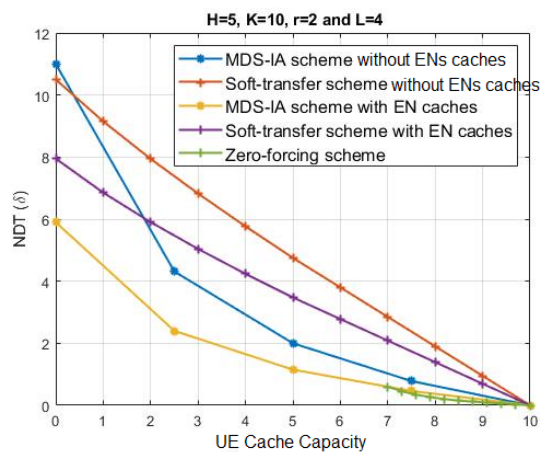
(a) Fronthaul multiplexing gain $\rho = 0.05$.(b) Fronthaul multiplexing gain $\rho = 20$.(c) Fronthaul multiplexing gain $\rho = \rho_{th} = 0.2353$.

Fig. 5: Comparison of the achievable NDT for a 5×10 RACN architecture with library $N = 10$ files, EN's cache size $\mu_T = .3$ and receiver connectivity $r = 2$ for the MDS-IA, soft-transfer and ZF schemes.

transfer scheme is minimal as it is derived based on an ideal fully cooperative delivery from the ENs. Therefore, when the fronthaul links are of high capacity, the performance of the soft transfer scheme becomes nearly optimal. On the other hand, when the fronthaul links are the bottleneck, latency can be reduced by delivering less information to the ENs, and this is achieved by MDS-IA. When the total cache size of one UEs and one EN is sufficient to store the entire library, i.e., $\mu_R \geq 0.7$, we observe from Fig. 5a that, when the fronthaul multiplexing gain is less than a threshold value ρ_{th} , i.e., $\rho < 0.2353$, the ZF scheme outperforms others. This is mainly because, in this scenario the ZF scheme does not use the fronthaul links, which constitute the

bottleneck.

VIII. CONCLUSIONS

We have studied centralized caching and delivery over a RACN with a specified network topology between the ENs and the UEs. We have proposed three schemes, namely the MDS-IA, soft-transfer, and ZF schemes. MDS-IA exploits MDS coding for placement and real IA for delivery. We have derived the achievable NDT for this scheme for an arbitrary cache capacity at the ENs and receiver connectivity of $r = 2$, and for an arbitrary receiver connectivity when the user cache capacities are above a certain threshold. The results show that increasing the receiver connectivity for the same number of ENs and UEs will reduce the NDT for a specific cache capacity at the UEs, while the amount of reduction depends on the fronthaul multiplexing gain, r . We also consider the soft-transfer scheme which quantizes and transmits coded symbols to each of the ENs over the fronthaul links, in order to implement ZF over the edge network. Finally, the ZF scheme is presented for an arbitrary value of r when the total cache size at one EN and one UE is sufficient to store the whole library. This allows all user requests to be satisfied by ZF from the ENs to the UEs without the participation of the cloud server. We have observed that when the total cache size of the UE and the EN is not sufficient to store the entire library, the MDS-IA scheme performs better when the fronthaul multiplexing gain is limited, while the soft-transfer scheme outperforms MDS-IA when the fronthaul multiplexing gain is high. On the other hand, when the total cache size of one UE and one EN is sufficient to store the entire library and the fronthaul capacity is below a certain threshold, ZF achieves the smallest NDT.

REFERENCES

- [1] N. Golrezaei, A. F. Molisch, A. G. Dimakis, and G. Caire, "Femtocaching and device-to-device collaboration: A new architecture for wireless video distribution," *IEEE Commun. Mag.*, vol. 51, no. 4, pp. 142–149, Apr. 2013.
- [2] M. Gregori, J. Gomez-Vilardebo, J. Matamoros, and D. Gunduz, "Wireless content caching for small cell and D2D networks," *IEEE J. Sel. Areas Commun.*, vol. 34, no. 5, pp. 1222–1234, May 2016.
- [3] E. Bastug, M. Bennis, and M. Debbah, "Social and spatial proactive caching for mobile data offloading," in *2014 IEEE International Conference on Communications Workshops (ICC)*, June 2014, pp. 581–586.
- [4] P. Blasco and D. Gunduz, "Multi-armed bandit optimization of cache content in wireless infostation networks," in *Proc. IEEE Int'l Symp. on Inform. Theory (ISIT)*, Honolulu, HI, Jun. 2014, pp. 51–55.
- [5] S. O. Somuyiwa, A. Gyrgy, and D. Gndz, "A reinforcement-learning approach to proactive caching in wireless networks," *IEEE Journal on Selected Areas in Communications*, vol. 36, no. 6, pp. 1331–1344, June 2018.
- [6] M. A. Maddah-Ali and U. Niesen, "Fundamental limits of caching," *IEEE Trans. on Inform. Theory*, vol. 60, no. 5, pp. 2856–2867, May 2014.

- [7] —, “Decentralized coded caching attains order-optimal memory-rate tradeoff,” *IEEE/ACM Trans. Netw.*, vol. 23, no. 4, August 2015.
- [8] M. Amiri, Q. Yang, and D. Gunduz, “Decentralized caching and coded delivery with distinct cache capacities,” *IEEE Trans. on Comms.*, vol. 65, no. 11, pp. 4657–4669, Nov 2017.
- [9] M. M. Amiri and D. Gunduz, “Cache-aided data delivery over erasure broadcast channels,” in *2017 IEEE Int’l Conf. on Comms. (ICC)*, May 2017, pp. 1–6.
- [10] S. S. Bidokhti, M. Wigger, and R. Timo, “Noisy broadcast networks with receiver caching,” *IEEE Trans. on Inform. Theory*, pp. 1–21, 2018.
- [11] M. A. Maddah-Ali and U. Niesen, “Cache-aided interference channels,” in *IEEE Int’l Symp. on Inform. Theory*, June 2015, pp. 809–813.
- [12] F. Xu, M. Tao, and K. Liu, “Fundamental tradeoff between storage and latency in cache-aided wireless interference networks,” *IEEE Trans. on Inform Theory*, vol. PP, no. 99, pp. 1–28, 2017.
- [13] J. P. Roig, D. Gunduz, and F. Tosato, “Interference networks with caches at both ends,” *IEEE Int’l Conf. on Comms.*, May 2017.
- [14] A. Sengupta, R. Tandon, and O. Simeone, “Fog-aided wireless networks for content delivery: Fundamental latency tradeoffs,” *IEEE Trans. on Inform. Theory*, vol. 63, no. 10, pp. 6650–6678, Oct 2017.
- [15] J. Koh, O. Simeone, R. Tandon, and J. Kang, “Cloud-aided edge caching with wireless multicast fronthauling in fog radio access networks,” in *IEEE Wireless Comms. and Networking Conf.*, Mar. 2017, pp. 1–6.
- [16] A. M. Girgis, O. Ercetin, M. Nafie, and T. ElBatt, “Decentralized coded caching in wireless networks: Trade-off between storage and latency,” in *IEEE Int’l Symp. on Inform. Theory*, Jun. 2017, pp. 2443–2447.
- [17] J. S. P. Roig, F. Tosato, and D. Gunduz, “Storage-latency trade-off in cache-aided fog radio access networks,” in *2018 IEEE Int’l Conf. on Comms. (ICC)*, May 2018, pp. 1–6.
- [18] S. M. Azimi, O. Simeone, and R. Tandon, “Content delivery in fog-aided small-cell systems with offline and online caching: An information theoretic analysis,” *Entropy*, vol. 19, no. 7, 2017.
- [19] N. Naderializadeh, M. A. Maddah-Ali, and A. S. Avestimehr, “Fundamental limits of cache-aided interference management,” *IEEE Trans. on Inform. Theory*, vol. 63, no. 5, pp. 3092–3107, May 2017.
- [20] N. Mital, D. Gunduz, and C. Ling, “Coded caching in a multi-server system with random topology,” in *2018 IEEE Wireless Communications and Networking Conference (WCNC)*, April 2018, pp. 1–6.
- [21] M. Ji, M. F. Wong, A. M. Tulino, J. Llorca, G. Caire, M. Effros, and M. Langberg, “On the fundamental limits of caching in combination networks,” in *IEEE Int’l Workshop on Signal Proc. Advances in Wireless Comms.*, Jun. 2015, pp. 695–699.
- [22] L. Tang and A. Ramamoorthy, “Coded caching for networks with the resolvability property,” in *IEEE Int’l Symp. on Inform. Theory*, July 2016, pp. 420–424.
- [23] A. A. Zewail and A. Yener, “Coded caching for combination networks with cache-aided relays,” in *IEEE Int’l Symp. on Inform. Theory*, Jun. 2017, pp. 2433–2437.
- [24] F. Xu and M. Tao, “Cache-aided interference management in partially connected wireless networks,” *ArXiv e-prints*, Aug. 2017.
- [25] A. Roushdy, A. S. Motahari, M. Nafie, and D. Gunduz, “Cache-aided fog radio access networks with partial connectivity,” in *IEEE Wireless Comms. and Networking Conf.*, April 2018, pp. 1–6.
- [26] J. Zhang and P. Elia, “Fundamental limits of cache-aided wireless bc: Interplay of coded-caching and csit feedback,” *IEEE Trans. on Inform. Theory*, vol. 63, no. 5, pp. 3142–3160, May 2017.
- [27] S. A. Jafar and S. Shamai, “Degrees of freedom region of the mimo x channel,” *IEEE Trans. on Inform. Theory*, vol. 54, no. 1, pp. 151–170, Jan 2008.

- [28] S. A. Jafar and M. J. Fakhreddin, "Degrees of freedom for the mimo interference channel," *IEEE Trans. on Inform. Theory*, vol. 53, no. 7, pp. 2637–2642, July 2007.
- [29] S. Lin and D. J. Costello, *Error Control Coding, Second Edition*, 2004.
- [30] A. S. Motahari, S. Oveis-Gharan, M. A. Maddah-Ali, and A. K. Khandani, "Real interference alignment: Exploiting the potential of single antenna systems," *IEEE Trans. on Inform. Theory*, vol. 60, no. 8, pp. 4799–4810, Aug 2014.
- [31] M. A. Maddah-Ali, "On the degrees of freedom of the compound miso broadcast channels with finite states," in *IEEE Int'l Symp. on Informa. Theory*, Jun. 2010, pp. 2273–2277.
- [32] O. Simeone, O. Somekh, H. V. Poor, and S. Shamai (Shitz), "Downlink multicell processing with limited-backhaul capacity," *EURASIP Journal on Advances in Signal Proc.*, vol. 2009, no. 1, Jun 2009.
- [33] Q. Yan, M. Cheng, X. Tang, and Q. Chen, "On the placement delivery array design for centralized coded caching scheme," *IEEE Trans. on Inform. Theory*, vol. 63, no. 9, Sep. 2017.
- [34] L. Tang and A. Ramamoorthy, "Coded caching schemes with reduced subpacketization from linear block codes," *IEEE Trans. on Inform. Theory*, April 2018.
- [35] J. Zhang, X. Lin, and X. Wang, "Coded caching under arbitrary popularity distributions," in *Infor. Theory and Applications Workshop (ITA)*, Feb 2015, pp. 98–107.